IMPROVING SINUSOIDAL FREQUENCY ESTIMATION USING A TRIGONOMETRIC APPROACH

Mathieu Lagrange, Sylvain Marchand

SCRIME – LaBRI, Université Bordeaux 1
351, cours de la Libération
F-33405 Talence cedex, France
firstname.name@labri.fr

Jean-Bernard Rault

France Télécom R&D
4, rue du Clos Courtel, BP 59
F-35512 Cesson Sevigné cedex, France
firstname.name@rd.francetelecom.com

ABSTRACT

Estimating the frequency of sinusoidal components is the first part of the sinusoidal analysis chain. Among numerous frequency estimators presented in the literature, we propose to study an estimator proposed in [1] known as the derivative algorithm. Thanks to a trigonometric interpretation of this frequency estimator, we are able to propose a new estimator which improves estimation performance for the frequencies close to the Nyquist frequency without any computational overload.

1. INTRODUCTION

Among numerous other applications, the estimation of the frequency of a sinusoidal signal is the first step of the sinusoidal analysis chain. Therefore, many methods have been proposed to achieve this goal. Some use the Short-Time Fourier Transform (STFT) as a starting point, often implemented by the Fast Fourier Transform (FFT). As a consequence, these estimators are often called "FFT-based" estimators.

A first class of these estimators considers some values of the power spectrum around a frequency component to fit a polynomial. The location of the maximum of this polynomial gives the precise frequency of the sinusoidal component [2, 3, 4]. In this paper, we will focus on a second class of estimators which explicitly use the phase of the FFT to estimate the frequency. Some estimators that belong to this class will be used to compare the estimator proposed in this article: the reassignment method [5], a phase-vocoder approach [6], and the derivative estimator [1].

It is proposed in [7, 8] to consider the signal derivative to obtain a precise estimation of the frequency of a sinusoidal component. Next, an improvement of this estimator is given in [1]. This new estimator – also called the derivative estimator – has been compared to existing frequency estimators in [9, 10]. In the last publication, the authors underline a potential defect: the performance of the derivative estimator decreases when the frequency to be estimated gets close to the Nyquist frequency.

In Section 2, we study the relationship between the amplitudes of a single sinusoidal component at two different moments. We are then able to propose two estimators of the frequency of a single sinusoid. These estimators are extended in Section 3 to the case of the estimation of the frequencies of multiple sinusoidal components. We will show that the first is identical to the derivative estimator that performs nicely in the low-frequency region and badly in the high-frequency one. The second estimator shows symmetrical properties as it performs nicely in the high-frequency region and badly in the low-frequency one. A new estimator, which is a combination of these two estimators, is then proposed. As detailed in Section 4, this new estimator still requires only the computation of two FFT.

Next, this new estimator is compared in Section 5 to existing phase-based methods and to the Cramér-Rao Bound (CRB). Both complex and real tones are used to compare these estimators.

2. ESTIMATING THE FREQUENCY OF A SINUSOID

In this section, we propose to study the relationship between the amplitudes of a sinusoidal signal at two different moments. Let s be a cosine signal with amplitude a and frequency $\omega = 2\pi f$ in radians per seconds (f in Hz) at two different times t and $t-\Delta$:

$$s(t) = a\cos(\omega t+\phi) \quad (1)$$
$$s(t-\Delta) = a\cos(\omega(t-\Delta)+\phi) \quad (2)$$

The difference and the summation of this signal at t and $t-\Delta$ can be written as:

$$s(t)-s(t-\Delta) = a'\cos(\omega t+\phi') \quad (3)$$
$$s(t)+s(t-\Delta) = a''\cos(\omega t+\phi'') \quad (4)$$

with a' and a'', two amplitudes:

$$a' = 2a\sin(\omega\Delta/2) \quad (5)$$
$$a'' = 2a\cos(\omega\Delta/2) \quad (6)$$

and ϕ' and ϕ'', two phases:

$$\phi' = \phi+\omega\Delta/2 \quad (7)$$
$$\phi'' = \phi-\omega\Delta/2+\pi \quad (8)$$

It follows that:

$$\frac{a'}{a} = 2\sin(\omega\Delta/2) \quad (9)$$
$$\frac{a''}{a} = 2\cos(\omega\Delta/2) \quad (10)$$

Two frequency estimators can be derived from Equations 9 and 10. These two estimators f^- and f^+ consider respectively the subtraction and the addition of the signal s at times t and $t-\Delta$:

$$f^- = \frac{1}{\pi\Delta}\arcsin\left(\frac{a'}{2a}\right) \quad (11)$$
$$f^+ = \frac{1}{\pi\Delta}\arccos\left(\frac{a''}{2a}\right) \quad (12)$$

These equations show that the frequency of a sinusoidal signal can be estimated using the amplitude of the signal and those of so-called "difference" and "sum" signals computed using the signal and its delayed version.

2.1. Discrete-Time Signals

In the case of discrete-time signals, the two frequency estimators f^- and f^+ can be easily implemented using a one-sample delay, i.e. by setting $\Delta = 1/F_s$, where F_s is the sampling frequency. In that case, Equations 1, 3, and 4 become:

$$s(n) = a\cos\left(\frac{2\pi}{F_s} fn\right) \tag{13}$$

$$\begin{array}{rcccl} s^-(n) & = & s(n)-s(n-1) & = & a'\cos\left(\frac{2\pi}{F_s} fn+\phi'\right) \\ s^+(n) & = & s(n)+s(n-1) & = & a''\cos\left(\frac{2\pi}{F_s} fn+\phi''\right) \end{array} \tag{14}$$

Equations 11 and 12 show that f^- and f^+ are based on the calculation of amplitude ratios, a'/a and a''/a. The problem is now to evaluate these amplitudes. If we consider that the signal under test (i.e. for which the frequency is being estimated) is locally stationary, e.g. for a duration corresponding to N samples, then a good estimator of the amplitudes is based on the variance calculation of s, s^-, and s^+ (which are all zero-mean signals):

$$\begin{array}{rcccl} \mathrm{var}(s) & = & \overline{s^2} & = & \frac{1}{N}\sum_{n=0}^{N-1} s(n)^2 \simeq a^2/2 \\ \mathrm{var}(s^-) & = & \overline{s^{-2}} & = & \frac{1}{N}\sum_{n=0}^{N-1} s^-(n)^2 \simeq a'^2/2 \\ \mathrm{var}(s^+) & = & \overline{s^{+2}} & = & \frac{1}{N}\sum_{n=0}^{N-1} s^+(n)^2 \simeq a''^2/2 \end{array}$$

so that:

$$a \simeq \sqrt{2\,\mathrm{var}(s)},\ a' \simeq \sqrt{2\,\mathrm{var}(s^-)},\ \text{and}\ a'' \simeq \sqrt{2\,\mathrm{var}(s^+)}.$$

Replacing a, a', and a'' in Equations 11 and 12, and considering $\Delta = 1/F_s$, the two estimators become:

$$f^- = \frac{F_s}{\pi}\arcsin\left(\frac{\sqrt{\mathrm{var}(s^-)}}{2\sqrt{\mathrm{var}(s)}}\right) \tag{15}$$

$$f^+ = \frac{F_s}{\pi}\arccos\left(\frac{\sqrt{\mathrm{var}(s^+)}}{2\sqrt{\mathrm{var}(s)}}\right) \tag{16}$$

2.2. Behaviors of the Estimators

The behaviors of the two estimators f^- and f^+ above have been analyzed for single-tone signals of constant frequencies. The sampling frequency has been set to $F_s = 44100$ Hz and the tone frequencies ranged from 0 to the Nyquist frequency ($F_s/2$) by step of 10 Hz. We set here $N = 2048$ for the practical experiments. The results of the simulation are represented on Figure 1. We can observe that the estimation error of f^- increases as the frequency of the analyzed signal grows. On contrary, the estimation error of f^+ increases as the frequency gets close to 0.

The behaviors of these two estimators are closely linked to the properties of the mathematical functions arcsin and arccos used in Equations 11 and 12. These functions are not linear transfer functions. If the argument gets close to 1, a small error will lead to a non-negligible error on the estimated frequency.

Moreover, the argument of the arcsin function used in Equation 11 leads to 1 for the Nyquist frequency and the argument of the arccos function used in Equation 12 leads to 1 for the frequency 0.

It is then useful to consider the f^- estimator if the frequency of the analyzed signal is below $F_s/4$ and to consider the f^+ estimator otherwise. By doing so, the influence of errors is minimized.

Since we do not have any information concerning the approximative frequency of s, we arbitrarily favor f^-:

$$f^{\pm} = \begin{cases} f^+ & \text{if } f^- > F_s/4 \text{ and } f^+ > F_s/4 \\ f^- & \text{otherwise} \end{cases} \tag{17}$$

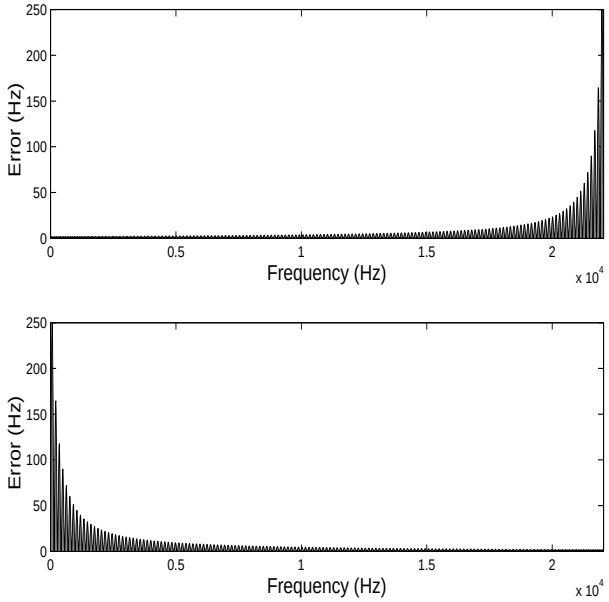

Figure 1: *On top, estimation error of f^- versus the frequency of the analyzed sinusoidal signal. At bottom, estimation error of f^+. It appears that the errors of these two estimators are symmetrically distributed around frequency $F_s/4$.*

2.3. Influence of Noise

To study the influence of noise on these estimators, we add a Gaussian noise y to a constant-frequency cosine signal x (see Equation 13), the resulting signal being:

$$s(n) = x(n) + y(n)$$

The Signal-to-Noise Ratio (SNR) is defined as the ratio between the energy of the sinusoid and the energy of the noise, in dB scale. For zero-mean signals like x or y (and s), the variance can be substituted to the energy, thus we have:

$$\mathrm{SNR} = 10\log_{10}\left(\frac{\mathrm{var}(x)}{\mathrm{var}(y)}\right) \tag{18}$$

As can be seen on Figure 2, the $f^{\pm}$ estimator gives good results for SNR above 40 dB. Below 40 dB, a bias can be observed, i.e. the estimated frequency gets "attracted" to a given frequency, in our case $F_s/4$. Indeed, at very low SNR we get:

$$\mathrm{var}(s) \simeq \mathrm{var}(y) \ \text{ and } \ \mathrm{var}(s^+) \simeq \mathrm{var}(s^-) \simeq 2\mathrm{var}(y)$$

and it follows, from Equations 15 and 16, that the estimated frequencies are then:

$$\begin{array}{rcccl} f^+ & = & \frac{F_s}{\pi}\arccos\left(\frac{1}{\sqrt{2}}\right) & = & F_s/4 \\ f^- & = & \frac{F_s}{\pi}\arcsin\left(\frac{1}{\sqrt{2}}\right) & = & F_s/4 \end{array} \tag{19}$$

3. ESTIMATING THE FREQUENCY OF MULTIPLE SINUSOIDS

The estimators studied in the previous section are limited to the analysis of only one sinusoid. Yet, most musical signals contain

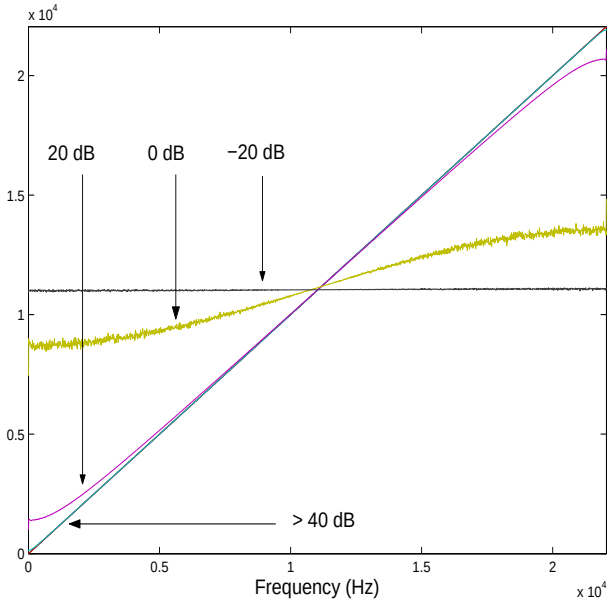

Figure 2: *Frequency estimated using $f^{\pm}$ defined in Equation 17 for a cosine and Gaussian noise mixture of given SNR, versus the frequency of the cosine.*

multiple frequency components. To estimate the frequencies of these components using the same principles, we must estimate the amplitude, the amplitude of the "difference" signal, and the amplitude of the "sum" signal of each component.

Let s be a signal made up with P sinusoidal components:

$$\begin{aligned} s(n) &= \sum_{p=1}^{P} s_p(n) \\ s_p(n) &= a_p \cos\left(\frac{2\pi}{F_s} f_p n + \phi_p\right) \end{aligned}$$

To estimate the frequencies f_p, we define:

$$\begin{array}{ccccc} s^-(n) & = & s(n)-s(n-1) & = & \sum_{p=1}^{P} s_p^-(n) \\ s^+(n) & = & s(n)+s(n-1) & = & \sum_{p=1}^{P} s_p^+(n) \end{array}$$

where s_p^- and s_p^+ are sinusoidal components of frequency f_p. It can be shown that each frequency f_p can be estimated using the following equations:

$$f_p^- = \frac{F_s}{\pi} \arcsin\left(\frac{a'_p}{2a_p}\right) \quad \text{and} \quad f_p^+ = \frac{F_s}{\pi} \arccos\left(\frac{a''_p}{2a_p}\right)$$

where a_p, a'_p, and a''_p are respectively the amplitudes of s_p, s_p^-, and s_p^+. To estimate these amplitudes, the analyzed signal s is windowed and a Discrete Fourier Transform (DFT) of size N is applied. The (periodic) Hann window will be used implicitly in the remainder of the paper, prior to every DFT, see for example [1] for a discussion. The size of the DFT is chosen so that the absolute difference of the frequencies of two components is at least F_s/N. In this case, each component s_p, s_p^-, and s_p^+ will give rise to a local maximum located at the DFT index k_p so that:

$$\frac{(k_p-0.5)F_s}{N} < f_p < \frac{(k_p+0.5)F_s}{N}$$

It can be shown that:

$$|S[k_p]| = Ka_p,\ |S^-[k_p]| = Ka'_p, \text{ and } |S^+[k_p]| = Ka''_p$$

with

$$K = \frac{1}{2}\left|W\left(f_p - \frac{k_p F_s}{N}\right)\right|$$

where W is the spectrum of the analysis window w used in combination with the Fourier transform (see [9]). The frequency estimators of f_p are then:

$$f_p^- = \frac{F_s}{\pi} \arcsin\left(\frac{|S^-[k_p]|}{2|S[k_p]|}\right) \tag{20}$$

$$f_p^+ = \frac{F_s}{\pi} \arccos\left(\frac{|S^+[k_p]|}{2|S[k_p]|}\right) \tag{21}$$

By setting

$$\begin{array}{ccccc} S^-[k] & = & \mathrm{DFT}[s(n)-s(n-1)] & = & S^1[k]/F_s \\ S[k] & = & \mathrm{DFT}[s(n)] & = & S^0[k] \end{array}$$

where S^m is the spectrum of m-th derivative of the signal s (S^0 being the spectrum of the signal itself), we find:

$$f_p^- = \frac{F_s}{\pi} \arcsin\left(\frac{1}{2F_s}\frac{|S^1[k_p]|}{|S^0[k_p]|}\right)$$

that is the estimator known as the derivative estimator proposed in [1]. The estimator f_p^+ is then an enhancement of the derivative estimator for the frequencies above $F_s/4$, see Equation 19.

Thanks to the spectral estimation available using the DFT of the signal, we can take advantage of the index of the local maximum to choose between the two estimators f_p^- and f_p^+:

$$\hat{f}_p = \begin{cases} f_p^- & \text{if } k_p < N/4 \\ f_p^+ & \text{otherwise} \end{cases} \tag{22}$$

4. IMPLEMENTATION

The use of the estimator defined in Equation 22 requires the computation of three DFT, see Equations 20 and 21. Yet, it can be noted that:

$$\begin{array}{ccccc} S^-[k] & = & \mathrm{DFT}[s^-(n)] & = & \mathrm{DFT}[s(n)]-\mathrm{DFT}[s(n-1)] \\ S^+[k] & = & \mathrm{DFT}[s^+(n)] & = & \mathrm{DFT}[s(n)]+\mathrm{DFT}[s(n-1)] \\ S^0[k] & = & \mathrm{DFT}[s(n)] & & \end{array}$$

so that only two DFT are needed:

$$S_0[k] = \mathrm{DFT}[s(n),\cdots,s(n+N-1)]$$

and

$$S_{-1}[k] = \mathrm{DFT}[s(n-1),\cdots,s(n+N-2)]$$

This way, for each local maximum with index k_p of the power spectrum $|S^0|$ ($S^0 = S_0$), the estimated frequency is:

$$\hat{f}_p = \begin{cases} \frac{F_s}{\pi} \arcsin\left(\frac{|S_0[k_p]-S_{-1}[k_p]|}{2|S_0[k_p]|}\right) & \text{if } k_p < N/4 \\ \frac{F_s}{\pi} \arccos\left(\frac{|S_0[k_p]+S_{-1}[k_p]|}{2|S_0[k_p]|}\right) & \text{otherwise} \end{cases} \tag{23}$$

To generate the contour plot of Figure 3, we used the protocol detailed in Section 5.1. We can observe that using the proposed estimator, the precision of the estimator is roughly independent of the frequency of the analyzed complex exponential. The performance of this new estimator will be deeply studied and compared in the next section.

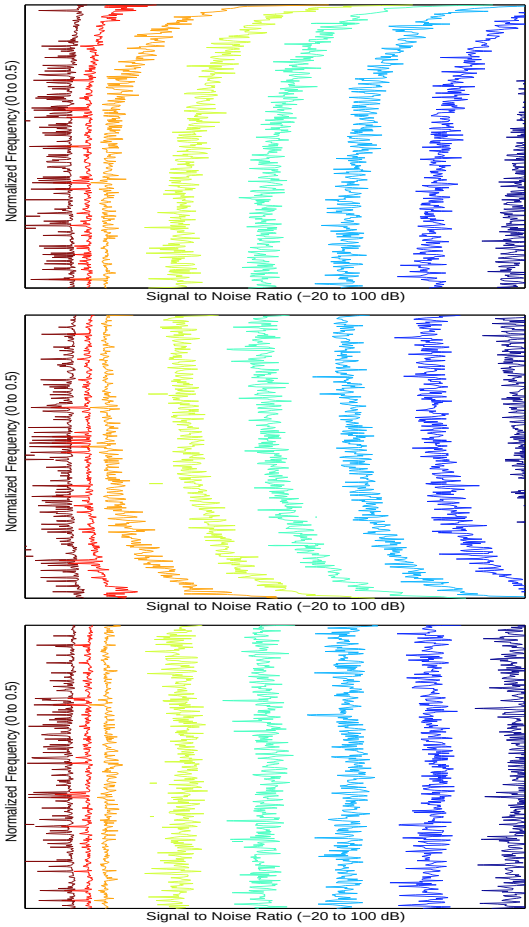

Figure 3: *Level curves of the frequency error versus the SNR and the frequency of the analyzed complex exponential for three estimators: f_p^- defined in Equation 20 (equivalent to the derivative estimator) on top, f_p^+ defined in Equation 21 in the middle, and f_p defined in Equation 23 at bottom. The level curves grow from the right to the left.*

5. PERFORMANCE

The performance of the proposed estimator is compared to the performances of some phase-based methods of the same computational order.

The reassignment method [5] uses the knowledge of the analytic first derivative w' of the analysis window w in order to adjust the frequency inside the DFT bin. For a local maximum located at index k_p, the reassigned frequency is computed as follows:

$$\hat{f}_r = k_p \frac{F_s}{N} - \Im\left(\frac{S_{w'}(k_p)}{S_w(k_p)}\right)\frac{F_s}{2\pi}$$

where S_w and $S_{w'}$ are the spectra of s using the analysis windows w and w', respectively.

The phase-vocoder approach [6] uses the phase difference between two successive short-term spectra in order to estimate the frequency. Given two successive spectra S_h and S'_h, computed with an overlap of $N-1$ samples, the estimated frequency of a local maximum at index k_p is:

$$\hat{f}_v = \frac{F_s}{2\pi}(\angle_u(S'_h(k_p)) - \angle(S_h(k_p)))$$

where $\angle_u(S'_h)$ is the unwrapped version of $\angle(S'_h)$ (the phase of S'_h), with respect to $\angle(S_h)$, the phase of the preceding spectrum.

For the sake of simplicity, we consider normalized frequencies in our experiments. We now use a 4-kHz sampling frequency and frames of $N = 128$ samples. The SNR ranges from -20 dB to 100 dB. We evaluate 400 different frequencies in the considered range. For the limited frequency range, the lower bound is set to 0.24 and the upper bound to 0.26 (normalized frequencies). For the whole frequency range, the lower bound is set to 0 and the upper bound to 0.5. These bounds are exclusive, so that the first evaluated frequency in the entire range is 0.0025. For each frequency, 30 different phases are evaluated from 0 to 2π. At each evaluation, the noise is randomized. For all the tested methods, the detection is operated by picking the greatest local maximum in the power spectrum.

An interesting element to compare with is the Cramér-Rao Bound (CRB), defined as the limit to the best possible performance achievable by an estimator given a dataset.

5.1. Complex Case

We consider a complex exponential x (of amplitude 1) in a Gaussian complex noise y:

$$\begin{aligned} x(n) &= \exp(j\omega n + \Phi) \\ y(n) &= 10^{-\mathrm{SNR}/20} z(n) \end{aligned}$$

where ω is the frequency (in radians per sample) and z is a Gaussian noise of variance 1. The variance of signal part x is 1, and the variance of the noise part y is $\mathrm{var}(y) = \sigma^2 = 10^{-\mathrm{SNR}/10}$. The analyzed signal is $s = x + y$.

For the case of the estimation of the frequency ω of a complex exponential in noise, the lower Cramér-Rao bound is [11]:

$$\mathrm{var}(\hat{\omega}) \geq \frac{6\sigma^2}{a^2 N(N^2-1)} = \frac{6}{N(N^2-1)}\, 10^{-\mathrm{SNR}/10} \qquad (24)$$

where a is the amplitude of the exponential (here $a = 1$), and the SNR is given by Equation 18. We can easily show that, in the log scales, the CRB in function of the SNR is a line of slope -1.

As will be detailed later, the performance of the tested estimators may depend on the frequency of the analyzed exponential, whether this frequency is close to 0 or the Nyquist frequency or not.

To first evaluate these estimators with at least a minimum influence of these frequency bounds, we compare the methods in the limited frequency range located around the 0.25 normalized frequency.

As asserted in [10], all the methods seem to perform similarly, see Figure 4. A bias can be observed for the reassignment. For a single exponential, it may be removed [12]. In this case, the reassignment performs as the phase-vocoder estimator, slightly better than the derivative estimator and the proposed estimator.

When the entire frequency range is considered, the derivative method performs badly, see Figure 5(a). This can be explained by the lack of precision in the high-frequency region, see Figure 5(b).

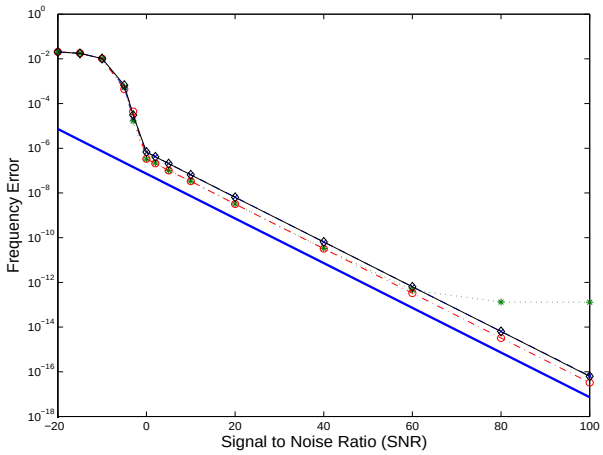

Figure 4: *Performance comparison of several estimators for the analysis of a complex exponential signal with frequency lying in the limited (normalized) frequency range* $]0.24, 0.26[$*: the reassignment method (dotted line with *), the phase-vocoder estimator (dash-dotted line with o), the derivative estimator (dashed line with x), and the proposed estimator (solid line with* $\diamond$*). The CRB is plotted with a double solid line.*

5.2. Real Case

Musical applications usually considers real sinusoids rather than complex exponentials. We then consider the signal $s = x + y$ made of a sinusoid x (of amplitude 1) in a Gaussian noise y:

$$\begin{aligned} x(n) &= \sin(\omega n + \Phi) \\ y(n) &= \frac{1}{\sqrt{2}} 10^{-\mathrm{SNR}/20} z(n) \end{aligned}$$

where ω is the frequency (in radians per sample) and z is a Gaussian noise of variance 1. We use the $1/\sqrt{2}$ normalizing factor to ensure the validity of Equation 18, because in the real case the variance of the sinusoid is $1/2$, while we still consider, by definition, $\mathrm{var}(y) = \sigma^2$.

For the case of the estimation of the frequency ω of a real sinusoid in noise, the lower Cramér-Rao bound is shown to be [13]:

$$\mathrm{var}(\hat{\omega}) \geq \frac{24\sigma^2}{a^2 N(N^2-1)} = \frac{12}{N(N^2-1)} 10^{-\mathrm{SNR}/10} \qquad (25)$$

where a is the amplitude of the sinusoid (here $a = 1$), and the SNR is given by Equation 18.

The spectrum of a real sinusoid is made of two Dirac's impulses, one located at frequency ω and the other at $-\omega$, and the spectrum of the sampled signal is F_s-periodic. As a consequence, the more the frequency of the analyzed sinusoid is close to 0 or $F_s/2$, the more the interference between the two complex exponentials is pronounced. This can greatly disturb the estimators, thus changing their relative performances in the real case.

Therefore, when the limited frequency range is considered (see above), the results are equivalent to the complex case, see Figure 6. If the whole frequency range is considered, the performances are limited by the interference phenomenon, so that the squared error is held asymptotically constant at SNR higher than 10 dB, see Figure 7(a). The phase-vocoder and reassignment methods perform equally at high SNR. The proposed estimator performs slightly better than both of them, and much better than the original derivative method. Thus, the proposed estimator appears to be the best estimator for the analysis of real signals over a wide range of frequencies.

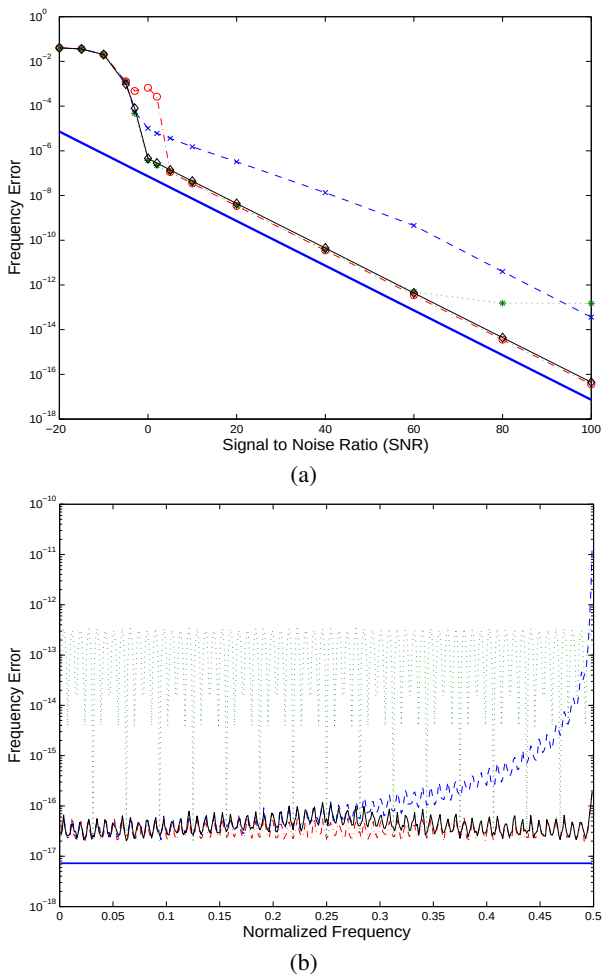

Figure 5: *On top, performance comparison of the tested estimators for the analysis of a complex exponential signal with frequency lying in the whole (normalized) frequency range* $]0, 0.5[$*: the reassignment method (dotted line with *), the phase-vocoder estimator (dash-dotted line with o), the derivative estimator (dashed line with x), and the proposed estimator (solid line with* $\diamond$*). The CRB is plotted with a double solid line. The prominent "bump" observed for the phase-vocoder at low SNR is due to the poor performance of this estimator at very low frequencies. At bottom, performance of the tested estimators at SNR=100 dB versus the frequency of the analyzed exponential (symbols are not plotted here for the sake of clarity).*

These results can be explained by properties of the tested estimators depending on the frequency of the analyzed sinusoid, see Figure 7(b). The phase-vocoder method is imprecise in the low-frequency region, as the derivative method is in the high-frequency one, and the bias of the reassignment method prevents this method to achieve good performance in the mid-frequency region.

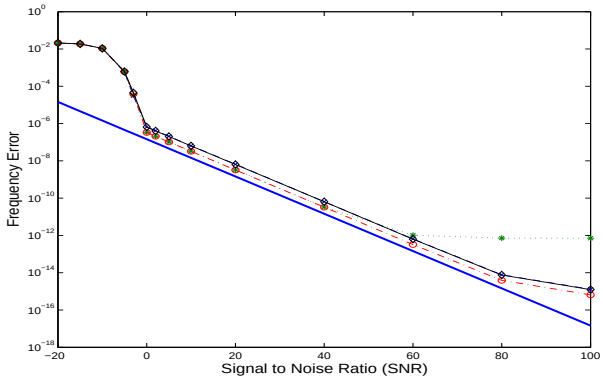

Figure 6: *Performance comparison of the tested estimators for the analysis of a real sinusoidal signal with a frequency lying in the limited (normalized) frequency range* $]0.24, 0.26[$.

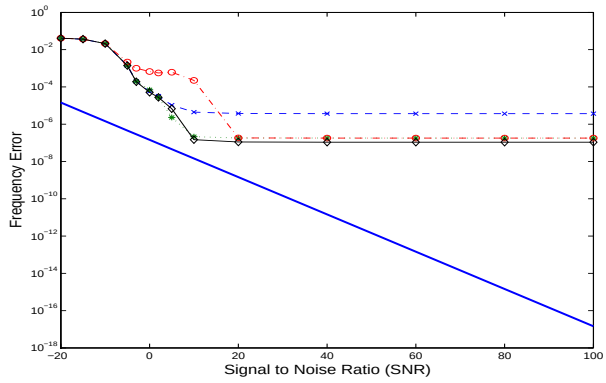

(a)

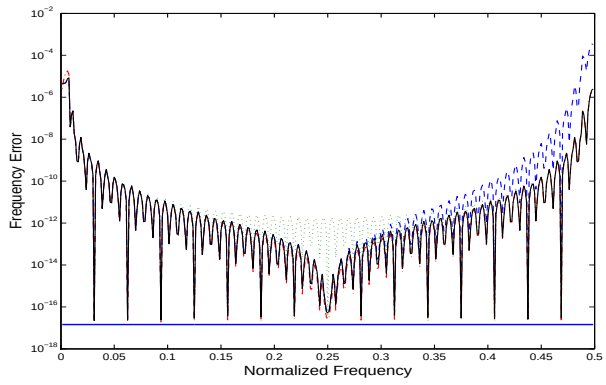

(b)

Figure 7: *On top, performance comparison of the tested estimators for the analysis of a real sinusoidal signal with frequency lying in the whole (normalized) frequency range* $]0, 0.5[$. *Again, the prominent "bump" observed for the phase-vocoder at low SNR is due to the poor performance of this estimator at very low frequencies. At bottom, performance of the tested estimators at SNR*=100 *dB versus the frequency of the analyzed sinusoid (symbols are not plotted here for the sake of clarity).*

6. CONCLUSION

We have shown in this article that the estimation of the frequency of a sinusoidal signal can be achieved by considering the amplitude of this signal at different moments. This study allows us to give a trigonometric interpretation of the derivative estimator and explain the loss of precision of this estimator for signals with frequencies close to the Nyquist frequency. A new estimator of the same complexity is then proposed and compared to other known phase-based estimators. According to the presented tests, the proposed estimator appears to be the best phase-based estimator for the analysis of real sinusoids with a wide range of frequencies.

7. REFERENCES

[1] Sylvain Marchand, *Sound Models for Computer Music (analysis, transformation, synthesis)*, Ph.D. thesis, University of Bordeaux 1, LaBRI, December 2000.

[2] Thomas Grandke, "Interpolation Algorithms for Discrete Fourier Transforms of Weighted Signals," *IEEE Transaction on Instruments and Measurements*, vol. 32, no. 2, pp. 350–355, 1983.

[3] Malcolm D. Macleod, "Fast Nearly ML Estimation of the Parameters of Real or Complex Single Tones or Resolved Multiple Tones," *IEEE Transactions on Signal Processing*, vol. 46, no. 1, pp. 141–148, 1998.

[4] Xavier Serra, *Musical Signal Processing*, chapter Musical Sound Modeling with Sinusoids plus Noise, pp. 91–122, Studies on New Music Research. Swets & Zeitlinger, Lisse, the Netherlands, 1997.

[5] François Auger and Patrick Flandrin, "Improving the Readability of Time-Frequency and Time-Scale Representations by the Reassignment Method," *IEEE Transactions on Signal Processing*, vol. 43, pp. 1068–1089, May 1995.

[6] Daniel Arfib, Florian Keiler, and Udo Zölzer, *DAFx – Digital Audio Effects*, J. Wiley and Sons, 2002, chapter 9, pp. 299-372.

[7] Myriam Desainte-Catherine and Sylvain Marchand, "High Precision Fourier Analysis of Sounds Using Signal Derivatives," *Journal of the Audio Engineering Society*, vol. 48, no. 7/8, pp. 654–667, July/August 2000.

[8] Sylvain Marchand, "Improving Spectral Analysis Precision with an Enhanced Phase Vocoder using Signal Derivatives," in *Proc. DAFx*, Barcelona, November 1998, pp. 114–118.

[9] Florian Keiler and Sylvain Marchand, "Survey on Extraction of Sinusoids in Stationary Sounds," in *Proc. DAFx*, September 2002, pp. 51–58.

[10] Stephen W. Hainsworth and Malcom D. Macleod, "On Sinusoidal Parameter Estimation," in *Proc. DAFx*, September 2003, pp. 151–156.

[11] David C. Rife and Robert R. Boorstyn, "Single-Tone Parameter Estimation from Discrete-Time Observations," *IEEE Transactions on Information Theory*, vol. IT-20, pp. 591–598, 1974.

[12] Stephen W. Hainsworth and Malcom D. Macleod, "Time-Frequency Reassignment: Measures and Uses," in *Proceedings of the Cambridge Music Processing Colloquium*, 2003, pp. 36–39.

[13] Steven M. Kay, *Fundamentals of Statistical Signal Processing – Estimation Theory*, Signal Processing Series. Prentice Hall, 1993.